

Facile synthesis of symmetrical di([1,1'-biphenyl]-4-yl) phthalates *via* Pd catalyzed Suzuki-Miyaura coupling with comparative vibrational and NMR spectroscopic analysis using DFT

Muhammad Zubair^a, Adeel Mubarik^b, Abid Mahmood^c, Maria Sohail^a, Nasir Rasool^{a*}, Aqsa Kanwal^a, Gulraiz Ahmad^a

^a Department of Chemistry, Government College University Faisalabad, Faisalabad, 38000, Pakistan

^b School of Chemistry and Chemical Engineering, Nanjing University of Science and Technology, Nanjing 210094, People's Republic of China

^c Department of Pharmaceutical Chemistry, Government College University Faisalabad, Faisalabad 38000, Pakistan

Email: nasirrasool@qcuf.edu.pk

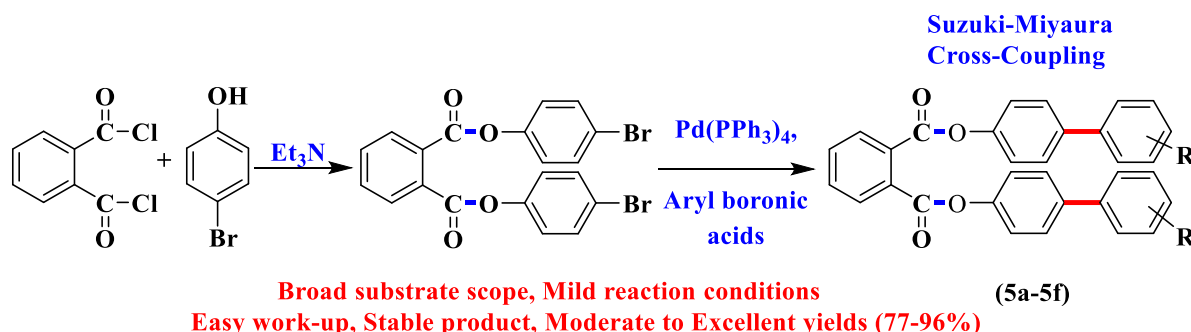
Received 12-28-2025

Accepted 05-01-2026

Published on line 05-09-2026

Abstract

In this study, the successful synthesis of bis(4-bromophenyl) phthalates through the reaction of phthaloyl chloride with 4-bromophenol and di([1,1'-biphenyl]-4-yl) phthalates (**5a-5f**) *via* a Suzuki-Miyaura coupling is described. DFT analysis was performed to deepen our understanding of the spectroscopic and electronic characteristics of the synthesized compounds. Conceptual DFT descriptors were studied in PBE0-D3BJ/def2-TZVP theory level for structure elucidation of the synthesized derivatives.



Keywords: Phthalic acid esters, di([1,1'-biphenyl]-4-yl) phthalates, Suzuki-Miyaura cross-coupling, density functional theory, comparative spectral studies; potential energy distribution

Introduction

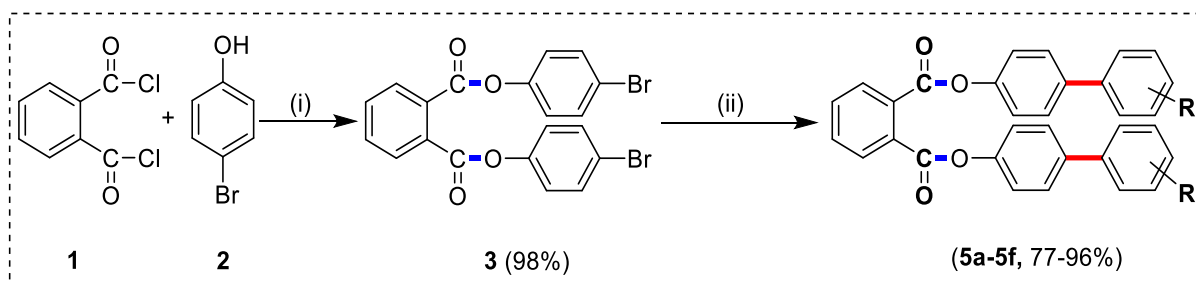
Phthalic acid esters (PAEs), extensively known as phthalates, are widely utilized as plasticizers to enhance the flexibility and durability of polymeric materials.¹ Typical representatives include butyl benzyl phthalate (BBP), dibutyl phthalate (DBP), di(2-ethylhexyl) phthalate (DEHP), diisononyl phthalate (DINP), and diisodecyl phthalate (DIDP).² Furthermore, phthalate derivatives have been explored in various functional materials (polymer electrolytes), where they can influence physicochemical properties.³⁻⁵ However, such application-oriented studies require system-level performance evaluation and will be explored in future studies. Aryl substitution of the phthalate framework provides a useful approach for examining structural and spectroscopic features. In this work, bis(4-bromophenyl) phthalate (**3**) was synthesized *via* the Schotten–Baumann reaction^{6,7} and subsequently converted to di([1,1'-biphenyl]-4-yl) phthalates (**5a–5f**) through Suzuki–Miyaura cross-coupling. The Suzuki–Miyaura reaction is a well-established and efficient method for C–C bond formation, enabling the introduction of biphenyl units under relatively mild conditions with broad functional group tolerance.⁸

To validate the wavenumber assignments of synthesized derivatives (**5a–5f**), DFT functional computations have also been executed. Moreover, the calculated spectra in terms of PED have been interpreted and according to PED study, each vibrational mode has been assigned.⁹⁻¹¹ PBE0-D3BJ/def2-TZVP theory level functional has previously exhibited an excellent conciliation between computational efficiency and accuracy of vibration spectra for large/medium-sized compounds.¹²⁻¹⁴ It is often observed that the frequencies of vibration calculated through computational quantum chemistry are frequently greater than experimentally determined alternates, hence empirical scaling parameters are commonly applied to improve the experimental vibrational patterns.¹⁵ These scaling factors are determined by mean deviation towards the predicted and experimentally determined frequencies, which depends on the computational method and basis sets used to perform computations.¹⁶⁻¹⁹ For this purpose, we used DFT studies to compute the geometrical properties and vibrational frequency spectrum of tailored bis(4-bromophenyl) phthalates in the ground state. We also measured the estimated values of vibrating experimentally determined frequencies. This will provide new insight into the molecular parameters and vibrational spectrum for further studies in the future.

In the present research work, we reported synthesis and comparison of arylated phthalates' theoretical and experimental spectral results (**5a–5f**). To current knowledge, no extensive quantum chemical computations or vibrational spectra of di([1,1'-biphenyl]-4-yl) phthalate analogs have been described previously. So, the current research aims to thoroughly investigate the vibrational spectra and identify the modes with increased wavenumber precision.

Results and Discussion

Bis(4-bromophenyl) phthalate (**3**) was synthesized by the reaction of phthaloyl chloride (**1**) and 4-bromophenol (**2**) in the presence of Et₃N as a base and DCM to obtain the desired product up to 98% at room temperature. Later, the Suzuki–Miyaura–coupling of bis(4-bromophenyl) phthalate (**3**) with several aryl boronic acids in the presence of the Pd(PPh₃)₄ (tetrakis(triphenylphosphine)palladium(0)) and K₃PO₄ as a mild base yielded targeted compounds (**5a–5f**) in fair to good yields (77–96%) (Scheme 1, Figure 1). The reaction optimization given below indicated that the K₃PO₄ and 1,4-dioxane/toluene are the best base and solvent, respectively (Table 1). It was observed that the electron-rich ring activating group gives a good yield, but the



Scheme 1. Synthesis of bis(4-bromophenyl) phthalate (**3**) and di([1,1'-biphenyl]-4-yl) phthalates (**5a-5f**).

Reagents and conditions: (i) **1** (1.0 eq.), **2** (2.1 eq.), Et₃N (2.5 eq.), in DCM (15 mL), stirred for 2 h. (ii) **3** (1 eq), Pd(PPh₃)₄ (7 mol%), K₃PO₄ (4.0 eq.), Aryl boronic acids (**4**) (2.2 eq.), 1, 4-dioxane/toluene (10 mL) (1:1), H₂O (1mL), reflux at 85-90 °C, 24 h.

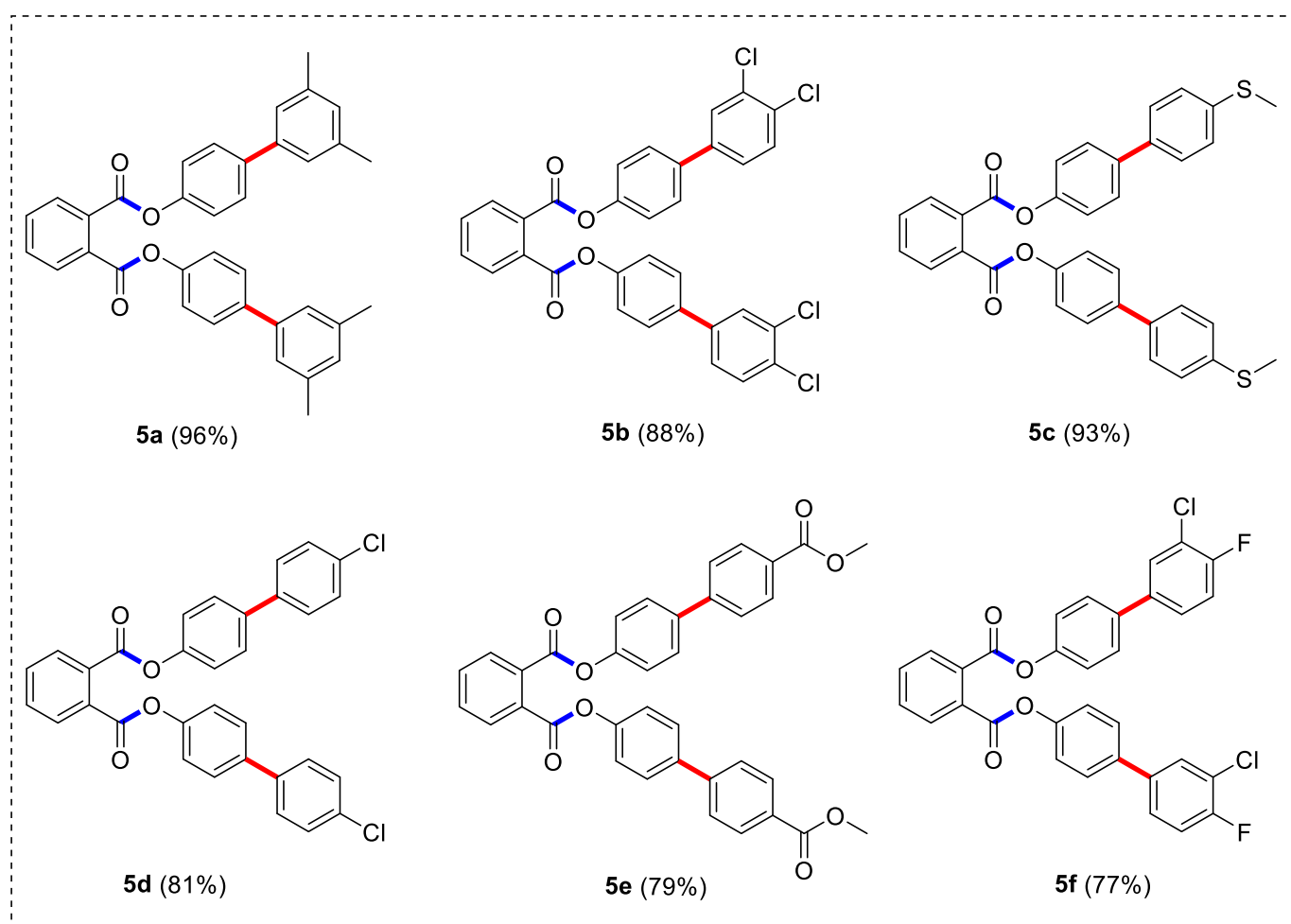


Figure 1. An overview of the structures of the di([1,1'-biphenyl]-4-yl) phthalates (**5a-5f**) and their percentage yields.

electron-rich boronic acid with two substitutions gives an excellent product yield (**5a**). However, it was also experimentally observed that the electron-poor substituted boronic acids give a very low yield of a product as in **5f**, due to electron-withdrawing substitution of a chloro group at *meta* and fluoro at *para* position leads to ring deactivation. Notably, it was also observed that increasing catalyst loading gives a higher yield. Increasing

the catalyst loading from 2.5 mol% to 5 mol% resulted in a moderate yield. Surprisingly, the use of K_3PO_4 with 5 mol% catalyst loading led to a significant increase in yield (93%). A further increase to 7 mol% afforded an excellent yield (96%). However, it was also observed that a moderately strong base as potassium phosphate (K_3PO_4), gives an excellent yield, compared to cesium carbonate (Cs_2CO_3), which may result from competing side reactions or base-dependent substrate decomposition,²⁰ ultimately leading to lower yield. Similarly, aqueous conditions using K_3PO_4 did not result in comparable yield losses, indicating that the effect is prompted by intrinsic base properties. Furthermore, mild base sodium carbonate (Na_2CO_3) gives a very low yield. Here, the effect of the solvent was never negligible. When toluene was used, moderate yields in the range of 51–57% were obtained. In contrast, switching to a 1,4-dioxane/toluene²¹ mixed solvent system resulted in a significant improvement in yield (72–96%) (Table 1).

Surprisingly, in Suzuki-Miyaura coupling, stable products were formed through optimized conditions. Notably, substrates bearing electron-donating groups, such as the dimethyl substitution in **5a** (96%) and the thiomethyl substitution in **5c** (93%), facilitated transmetalation (rate-determining step) more effectively. In contrast, substrates with electron-withdrawing groups, **5b** (88%), **5d** (81%), and **5f** (77%), or the ester group in **5e** (79%), gave comparatively slightly lower yields. Furthermore, no protodeboronation was observed, likely due to the carefully controlled temperature and optimized reaction parameters. The synthesized compounds (**5a–5f**) were purified from flash column chromatography. They were characterized by various spectroscopic techniques (1H -NMR and ^{13}C -NMR) and elemental analysis.

Table 1. Optimization of catalyst, solvents, and base for Suzuki-Miyaura coupling (**5a**)

Entry	Base	Catalyst loading	Solvents	Yield
1	Na_2CO_3	2.5 mol%	Toluene	51
2	Na_2CO_3	5 mol%	Toluene	54
3	Cs_2CO_3	2.5 mol%	Toluene	57
4	Cs_2CO_3	5 mol%	1,4-dioxane/toluene	72
5	K_3PO_4	5 mol%	1,4-dioxane/toluene	93
6	K_3PO_4	7 mol%	1,4-dioxane/toluene	96

Computational details

All calculations in the current research work were performed through DFT with the PBE0-D3BJ/def2-TZVP theory level as implemented in the Gaussian 09 program.^{22, 23} This basis set was chosen due to its reasonable balance between accuracy and computational cost for the system under investigation. Initially, the ground-state optimized geometries of the synthesized di([1,1'-biphenyl]-4-yl) phthalates (**5a–5f**) were calculated to ensure that the geometries correspond to stable configurations of the compounds (Figure 2). The optimized electronic structures obtained in this study relate to energy minima, as evidenced by the absence of imaginary frequencies in the vibrational frequency analysis. The electronic properties of the molecule by calculating the HOMO and the LUMO energies to examine the electronic structure and the molecule stability. The Molecular Electrostatic Potential (MEP) is also investigated to visualize the electron density distribution across the molecule's surface. Key reactivity descriptors were also determined to understand the molecule's chemical reactivity and polarity. Chemical potential was calculated providing further insight into the compound's stability. The spectroscopic features such as vibrational and nuclear magnetic resonance (NMR) spectra were also measured to compare with the experimental data. PED analysis, carried out with VEDA 4 program²⁴

facilitated the assignment of vibrational modes, supporting the understanding of molecular vibrations.^{25, 26} The ¹H NMR spectroscopic shifts (δ) of synthesized derivatives (**5a-5f**), were calculated from GIAO (gauge-independent atomic orbit) approach, where theoretically measured shifts were in good agreement with experimentally determined values. Furthermore, Conformational analysis was carried out by selected dihedral angle, as illustrated in Figure S1 and each dihedral angle (atoms mention in Figure S1) in steps of 30° over one complete rotation (0–360°) of compound **5a**. The energy value of all conformers of **5a** are given in Table S1 in supporting information. The combined use of computational and experimental methods in this study highlights the importance of DFT calculations in predicting molecular behavior and guiding future research in organic synthesis.

3.2 NMR Spectroscopy and GIAO-DFT Chemical Shift Analysis

NMR spectroscopy is the key method for identifying organic molecular structures. Quantum calculations precisely link computed chemical shifts to molecular structure.²⁷ Thus, applying theoretical approaches may strengthen confidence in describing structure of synthesized derivatives.²⁸ NMR spectroscopic calculations were done for all simulated molecules then compared with experimental NMR data. In Table 2, experimentally and theoretically calculated ¹H NMR spectroscopy data of synthesized derivative **5a** have been explained for comparison while the remaining compounds (**5b-5f**), ¹H NMR spectroscopy data are given in Supplementary data (Tables S2–S6). Mean absolute deviation can be expressed as mean absolute error, while root-mean-square deviation as root-mean-square error. Boltzmann-averaged values are given in respective tables which strongly correlate with experimentally determined data. It can be observed that the performance of NMR spectroscopy calculations of **5a** is very good, and MAE (mean absolute error) is only 0.43 ppm (Table 2).

Table 2. Comparison of experimentally determined and theoretically calculated ¹H NMR data of synthesized derivative **5a**

Carbon No.	Carbon Type	¹ H-NMR (δ , ppm) Experimentally determined	¹ H-NMR (δ , ppm) Computed theoretically	$\Delta\delta$, ppm
1	CH	8.04	7.45	0.59
2	CH	7.73	7.19	0.54
3	CH	7.67	7.21	0.46
4	CH	7.94	6.98	0.96
8	CH	7.51	6.83	0.68
9	CH	7.58	7.10	0.48
11	CH	7.58	7.18	0.40
12	CH	7.51	7.00	0.51
14	CH	7.27	6.90	0.37
16	CH	6.99	6.56	0.43
18	CH	7.27	6.78	0.49

Table 2. Continued

Carbon No.	Carbon Type	¹ H-NMR (δ , ppm) Experimentally determined	¹ H-NMR (δ , ppm) Computed theoretically	$\Delta\delta$, ppm
19	CH ₃	2.38	2.17	0.21
20	CH ₃	2.38	2.23	0.15
8'	CH	7.11	6.93	0.18
9'	CH	7.58	7.05	0.53
11'	CH	7.58	6.93	0.65
12'	CH	7.11	6.60	0.51
14'	CH	7.27	6.65	0.62
16'	CH	6.99	6.51	0.48
18'	CH	7.27	6.68	0.59
19'	CH ₃	2.38	2.11	0.27
20'	CH ₃	2.38	2.05	0.33
MAE (Mean Absolute Error) = 0.43				
RMSE (Root Mean Square Error) = 0.48				

Comparative IR and PED of compound 5a

The vibrational frequencies of the synthesized compounds were experimentally measured and compared with computationally calculated frequencies (both unscaled and scaled) and potential energy distribution (PED) values.²⁹ This validation process was crucial for assigning each vibrational frequency based on potential energy distribution (PED), allowing for a clearer interpretation of the molecular vibrations.³⁰ The comparison reveals strong agreement between experimental and calculated frequencies, with notable vibrations observed at C-H stretching 3013 cm⁻¹, 2916 cm⁻¹, 2851 cm⁻¹ (C-H stretching), 1735 cm⁻¹ (-O-C=O ester stretching), 1684 cm⁻¹ (C=O carbonyl stretch), C-C stretching and bending 1597 cm⁻¹, 1507 cm⁻¹. The PED analysis, which assigns specific vibrational modes, shows significant contributions for C-H stretching, C-C stretching, and bending modes, with higher PED values corresponding to dominant vibrations such as the C-H stretches (97%) and C=O stretches (89%) (Table 3). Noteworthy, the correlation between experimental and computational vibrational frequencies confirms the reliability of the theoretical model. Higher stability, indicated by a larger HOMO-LUMO energy gap (ΔE), corresponds to higher vibrational frequencies due to stronger bonding interactions. Conversely, smaller ΔE values suggest increased electron delocalization, leading to weaker bonds and lower vibrational modes. Since vibrational modes are influenced by electronic distribution, particularly molecular orbitals, the HOMO-LUMO gap analysis was conducted to explore further the electronic properties, mainly charge transfer, reactivity, and stability of synthesized compounds (**5a-5f**).

Table 3. Experimental and calculated Frequencies with PED% and vibrations of Compound **5a**

Experimental Frequencies (cm ⁻¹)	Calculated Frequencies		PED %	Vibrations
	Unscaled value (cm ⁻¹)	Scaled value (cm ⁻¹)		
3013	3266	3005	97	s (CH)
2916	3163	2910	64	s (CH)
2851	3053	2808	30	s (CH)
1735	1890	1739	89	s (COO)
1684	1866	1716	89	s (CO)
1597	1687	1552	29	s (CC)
1507	1684	1549	24	s (CC)
-	1660	1527	29	s (CC)
1479	1567	1442	19	b (HCC)
1395	1512	1391	12	s (CC)
1259.	1363	1254	13	s (CC)
-	1360	1252	14	s (CC)
1190	1292	1189	37	s (CO)
1161	1266	1164	20	s (CO)
1127	1239	1140	11	s (CC)
1038	1129	1038	30	b (HCC)
-	1127	1036	31	b (HCC)
877	930	855	16	t (HCCC)
849	921	847	22	t (HCCC)
803	879	809	11	b (CCC)
726	796	733	16	O (OCOC)
-	752	692	10	t (CCCC)

s=Stretching, t=Torsional, b=Bending, O= out of plane bending

FMO analysis

HOMO, LUMO, and energy gaps (ΔE) are employed to study various electronic features, reactivity, and tendency towards stability of molecules.¹⁹ The ΔE serves as a key indicator of stability, the larger the ΔE more stability and less reactivity of the compound while the opposite is true when ΔE is smaller. Arylated phthalates with diverse functional groups have a strong potential to modify the sites and ΔE (Figure 3). The reactivity features of any structure may be altered through inserting alternative functional substitutions onto their structural cores, ultimately changing their ΔE . The ΔE was found to range from 4.16 eV (**5c**) to 4.87 eV (**5e**). In

the series **5a–5f**, **5c** exhibits the lowest energy gap of 4.16 eV, indicating its least stability and highest reactivity due to thiomethyl substitution at a para position leads to electron delocalization and enhances charge transfer ability by increasing π -electron delocalization. In contrast, **5e** displays the highest ΔE of 4.87 eV, suggesting its highest stability and least reactivity. However, the theoretically calculated E_{LUMO} , E_{HOMO} , ΔE values of di([1,1'-biphenyl]-4-yl) phthalate (**5a–5f**) are enlisted in Table 4, and Figure 3.

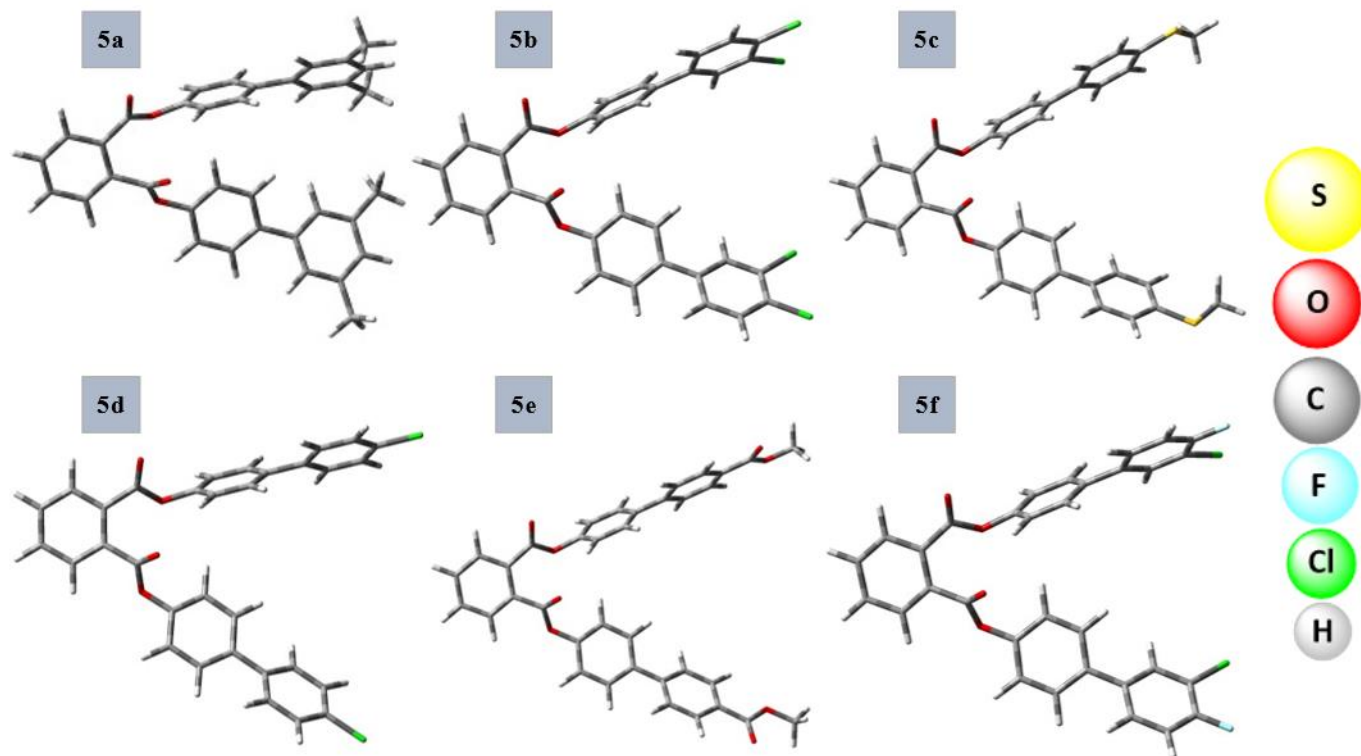


Figure 2. 3D Optimized structures of synthesized derivatives (**5a–5f**) by the PBE0-D3BJ/def2-TZVP theory level.

Table 4. Theoretically calculated values of E_{LUMO} , E_{HOMO} , $E_{\text{HOMO}}-E_{\text{LUMO}}$ gap (ΔE) of synthesized derivatives (**5a–5f**)

Compounds	E_{HOMO}	E_{LUMO}	ΔE
5a	-6.30	-1.65	4.65
5b	-6.57	-1.77	4.81
5c	-5.79	-1.63	4.16
5d	-6.47	-1.71	4.76
5e	-6.64	-1.77	4.87
5f	-6.56	-1.74	4.82

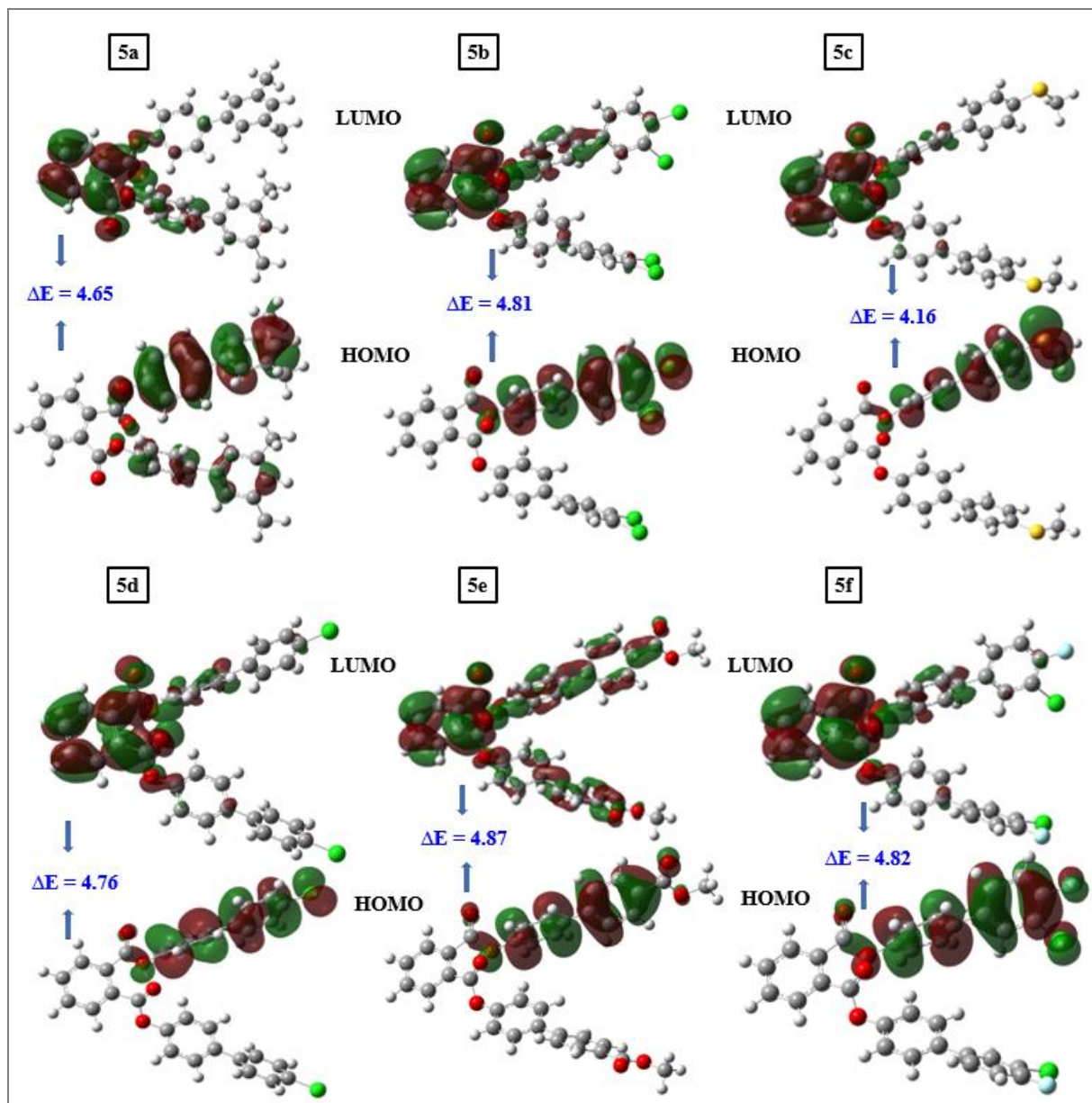


Figure 3. Molecular Orbitals (HOMO-LUMO) of arylated analogs of bis(4-bromophenyl) phthalates (**5a-5f**) calculated at PBE0-D3BJ/def2-TZVP level of theory.

Molecular electrostatic potential analysis (MESP)

MEP is highly valuable in analyzing molecular structure and its physiochemical parameter associations.^{31, 32} The molecular electrostatic potential can be used to calculate the reactive sites of molecules. Figure 4 depicts the MEP of each chemical. The color scheme for the MEP surface for partially negative charge or electron-rich is red color, for electron-deficient or partially positive charge is blue color, light blue for slightly electron-deficient zone, and yellow for slightly electron-rich region. The MEP clearly shows negative regions (red colored) that are focused around the compound's heteroatoms (nitrogen, oxygen, sulfur, and halogens). These sites are favorable for an electrophilic attack. The blue colored (positive regions) indicates the possible sites for a nucleophilic attack are localized around the aromatic benzene rings. MEP surfaces indicate the feasible sites readily available for the electrophilic and nucleophilic reaction pathways.

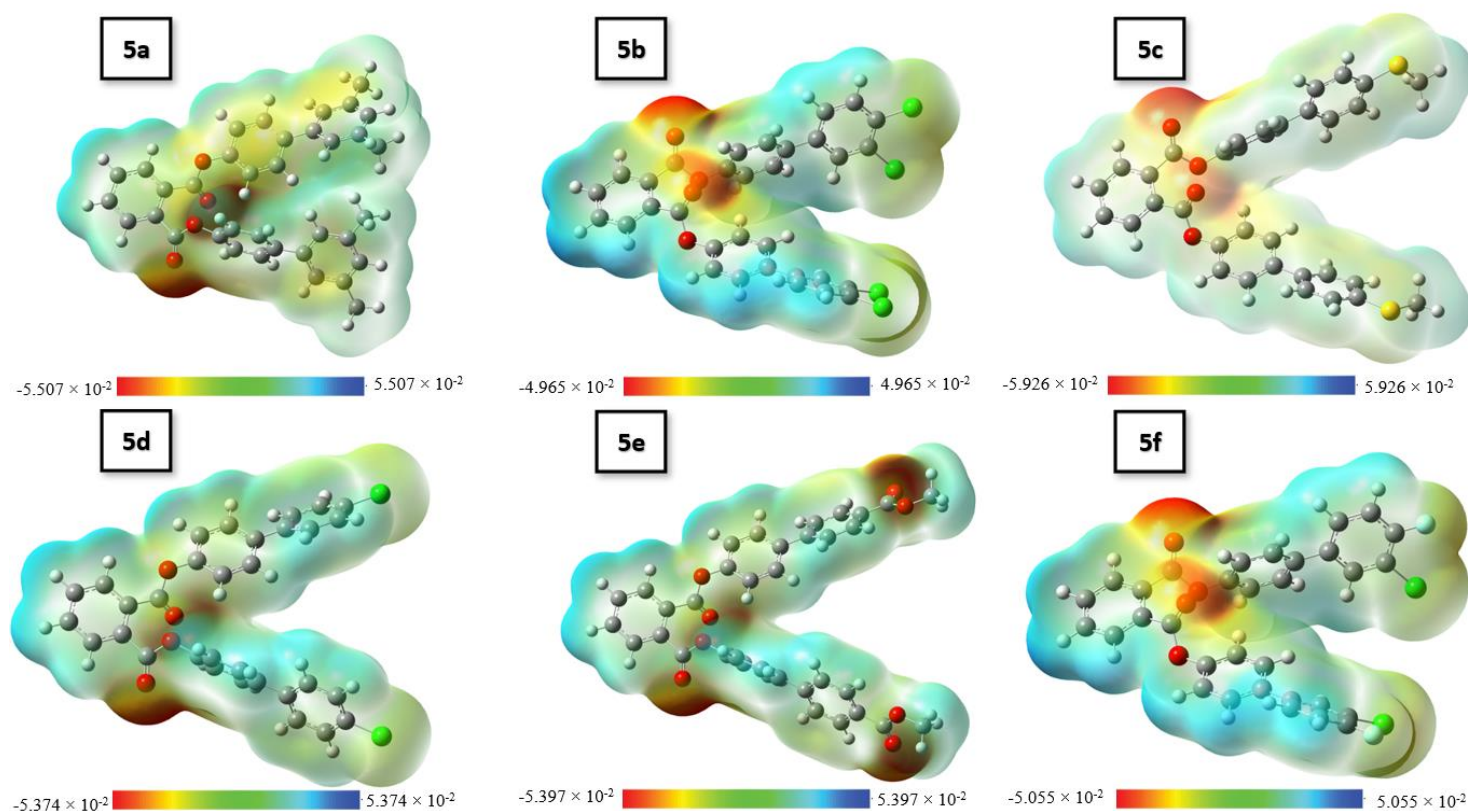


Figure 4. Molecular electrostatic potentials maps of (5a–5f).

Reactivity descriptors

The global reactivity descriptors derived from frontier orbital energies are summarized in Table 5. The ionization potential (IP) values range from 5.79 to 6.64 eV, while electron affinity (EA) varies between 1.63 and 1.77 eV, indicating relatively consistent electronic characteristics across the series. Among the studied compounds, **5c** exhibits the lowest IP (5.79 eV) and chemical hardness ($\eta = 2.08$ eV), along with the highest global softness ($S = 0.48$), suggesting comparatively higher reactivity and greater ease of charge transfer. In contrast, compounds such as **5e** and **5f** show higher hardness ($\eta \approx 2.41$ – 2.43 eV) and lower softness ($S \approx 0.41$), indicating increased stability and reduced reactivity.¹⁶ The electronegativity (χ) and electrophilicity index (ω) follow similar trends, with slightly higher values for **5e** and **5b**, suggesting a greater tendency to accept electrons. Overall, the small variation in these descriptors reflects that the electronic properties are primarily governed by the conjugated biphenyl–phthalate framework, with substituent effects introducing only moderate modulation. These trends are consistent with the delocalized π -system and support the observed stability of the synthesized derivatives. Electronegativity (χ), electrophilicity index (ω), chemical hardness (η), chemical potential (μ), and global softness (S) were determined using Eq. 1–5, which have been reported in many research studies^{18, 33, 34} and are reported in Table 5.

$$\chi = [\text{IP} + \text{EA}] / 2 = - [E_{\text{LUMO}} + E_{\text{HOMO}}] / 2 \quad (1)$$

$$\eta = [\text{IP} - \text{EA}] / 2 = - [E_{\text{LUMO}} - E_{\text{HOMO}}] / 2 \quad (2)$$

$$\mu = [E_{\text{LUMO}} + E_{\text{HOMO}}] / 2 \quad (3)$$

$$S = 1/\eta \quad (4)$$

$$\omega = \mu^2 / 2\eta \quad (5)$$

Table 5 Reactivity descriptors of all synthesized derivatives (**5a–5f**)

Compound	Electron Affinity (EA)	Ionization Potential (IP)	Electro-negativity (χ)	Electrophilicity (ω)	Chemical Potential (μ)	Global Hardness (η)	Global Softness (S)
5a	1.65	6.30	3.97	3.39	-3.97	2.33	0.43
5b	1.77	6.58	4.17	3.62	-4.17	2.40	0.41
5c	1.63	5.79	3.71	3.32	-3.71	2.08	0.48
5d	1.71	6.47	4.09	3.51	-4.09	2.38	0.42
5e	1.77	6.64	4.21	3.64	-4.21	2.43	0.41
5f	1.74	6.57	4.15	3.58	-4.15	2.41	0.41

Conclusions

Bis(4-bromophenyl) phthalate (**3**) was synthesized by treating with Phthaloyl chloride and 4-bromophenol, following synthesis of arylated phthalates (**5a–5f**) *via* SMC. The structural characterization of the synthesized compounds was comprehensively performed using a combination of experimental spectroscopic techniques, including nuclear magnetic resonance (NMR) and infrared (IR) spectroscopy, and supported by density functional theory (DFT) calculations. These approaches allowed us to confirm the identity and structure of the compounds, with the NMR chemical shifts and IR vibrational modes showing excellent agreement with experimental results. Thermodynamic and chemical parameters, such as HOMO and LUMO energy differences, were also calculated by computation to assess the stability and reactivity of the compounds. Most and least reactive compounds in the series (**5a–5f**) are identified by comparing energies to all compounds. **5c** exhibits the lowest ΔE of 4.16 eV, indicating its least stability in the synthesized series (**5a–5f**). In contrast, **5e** displays the highest ΔE gap of 4.87 eV, suggesting its highest stability. These calculations not only provided insights into the compounds' electronic properties but also highlighted the reactivity trends within the series. The molecular electrostatic potential maps identify active sites for electrophilic and nucleophilic attacks. The analysis of spectroscopic features, including vibrational (IR, PED%) and NMR spectroscopy, was performed and correlated with experimental data. Utilizing the VEDA 4 program for PED analysis allowed for the effective assignment of vibrational modes. The ^1H NMR spectroscopy shifts (δ) were calculated using the GIAO technique, yielding results that are consistent with experimental findings. Integrating computational and experimental methods comprehensively studies the molecules' synthesis, reactivity, and structural properties, which might increase their potential utility in diverse domains.

Experimental Section

General: FT-IR spectrum of synthesized compounds was found in the 4000–650 cm^{-1} ranges. Through KBr disc protocol, the FT-IR were recorded at 300 K at solid phase. Samples' infrared spectra were measured using a 1000 FT-IR Mattson spectrometer. Melting points of freshly synthesized derivatives (**5a–5f**) were calculated with B-540 (Buchi) equipment. Macklin China provided chemicals used in present study. The spectroscopic study employed the Advance III Bruker spectrometer to investigate the NMR spectra of yielded molecules in deuterated CDCl_3 . The J (coupling constant) has been taken in Hz, whereas δ (chemical shift) was determined in

ppm. To purify the synthesized derivatives (**5a-5f**), column chromatography with silica gel having mesh size 200-400 was employed. LECO CH micro analyzer (630-200-200 TruSpec) was utilized for elemental analysis.

Synthesis of bis(4-bromophenyl) phthalate (**3**)

Phthaloyl chloride (0.92 mL, 6.4 mmol, 1.0 eq.) was mixed with 4-bromophenol (2.32 g, 13.4 mmol, 2.1 eq.), after which 2.23 mL (2.5 eq.) of triethylamine was added dropwise at 0°C to the mixture. Then the reaction mixture was stirred in the presence of dichloromethane (DCM) as a solvent (15 mL) at room temperature for 2 h. The final product was obtained as pink crystals after workup by adding H₂O to the reaction mixture. The reaction mixture and water were extracted three times with 30 mL DCM. The lower layer was separated and dried with a rotary evaporator under reduced pressure. The target compound was characterized using NMR spectroscopy.

Synthesis of di([1,1'-biphenyl]-4-yl) phthalates (**5a-5f**)

The calculated amount of bis (4-phenylphthalate) (0.20 g, 0.42 mmol, 1 eq.), palladium catalyst in the form of tetrakis (triphenylphosphine) (0.03 g, 7 mol%), and 1,4-dioxane/toluene (10 mL) having a ratio (1:1) was taken in the Schlenk tube. The reaction was stirred for 30 min at room temperature in an inert atmosphere under argon. 2.2 eq. (0.46 mmol) of aryl boronic acid and 4.0 eq. (0.35 g, 1.68 mmol) of K₃PO₄ were added, and then 1 mL of distilled water was added to reaction mixture *via* using a syringe and then kept on refluxing at 85-90°C. The reaction was continuously monitored through TLC chromatography after every 3-4 h. The mixture was then filtered with the help of ethyl acetate and dried under reduced pressure with a rotary evaporator. Further, it was purified through column chromatography with a ratio of ethyl acetate/*n*-hexane (1:9). The purified product was then analyzed *via* ¹H-NMR and ¹³C-NMR spectroscopy.

Bis(4-bromophenyl) phthalate (**3**)

Yield: 98 %. Light pink crystals. mp: 194°C. IR (KBr) cm⁻¹: 3086 (C-H stretching), 1729, 1742 (O-C=O-stretching), 1638 (C=O stretching), 1479, 1442 (C=C stretching). ¹H NMR (400 MHz, CDCl₃) δ 7.96 (dd, *J* = 5.7, 3.3 Hz, 2H, Ar-H), 7.68 (dt, *J* = 7.3, 3.6 Hz, 2H, Ar-H), 7.52 – 7.48 (m, 4H, Ar-H), 7.10 (dd, *J* = 9.4, 2.6 Hz, 4H, Ar-H). ¹³C NMR (101 MHz, CDCl₃) δ 165.5, 149.7, 132.6, 132.1, 131.3, 129.6, 123.3, 119.4. Elemental Anal. Calcd. for C₂₀H₁₂Br₂O₄ (476.12): C, 50.45; H, 2.54% Found: C, 50.41; H, 2.57%.

Bis(3',5'-dimethyl-[1,1'-biphenyl]-4-yl) phthalate (**5a**)

Yield: 96%. White crystals. mp: 224-225 °C. IR (KBr) cm⁻¹: 3013, 2916, 2851 (C-H stretching), 1735 (O-C=O-stretching), 1684 (C=O stretching), 1597, 1507 (C=C stretching). ¹H NMR (400 MHz, CDCl₃) δ 8.04 – 7.94 (m, 2H, Ar-H), 7.73 – 7.67 (m, 2H, Ar-H), 7.58 (d, *J* = 8.7 Hz, 4H, Ar-H), 7.51 (dd, *J* = 8.8, 2.1 Hz, 2H, Ar-H), 7.30 – 7.24 (m, 4H, Ar-H), 7.11 (dd, *J* = 12.2, 8.9 Hz, 2H, Ar-H), 6.99 (s, 2H, Ar-H), 2.38 (s, 12H, 4CH₃). ¹³C NMR (101 MHz, CDCl₃) δ 166.0 (C=O), 150.0, 140.3, 139.5, 138.3, 132.6, 131.9, 129.7, 129.0, 128.3, 125.1, 123.4, 123.3, 121.7, 21.4. Elemental Anal. Calcd. for C₃₆H₃₀O₄ (526.63): C, 82.11; H, 5.73% Found: C, 82.09; H, 5.67%.

Bis(3',4'-dichloro-[1,1'-biphenyl]-4-yl) phthalate (**5b**)

Yield: 88%. Brown solids. mp: 224-226 °C. IR (KBr) cm⁻¹: 3031, 2958, 2919, 2844 (C-H stretching), 1721 (O-C=O-stretching), 1689 (C=O stretching), 1483 (C=C stretching). ¹H NMR (400 MHz, CDCl₃) δ 8.01 (dd, *J* = 5.7, 3.3 Hz, 2H, Ar-H), 7.76 – 7.66 (m, 2H, Ar-H), 7.63 (d, *J* = 2.2 Hz, 2H, Ar-H), 7.54 (d, *J* = 2.0 Hz, 4H, Ar-H), 7.48 (d, *J* = 8.3 Hz, 2H, Ar-H), 7.37 (dd, *J* = 8.4, 2.2 Hz, 2H, Ar-H), 7.31 (d, *J* = 8.6 Hz, 4H, Ar-H). ¹³C NMR (101 MHz, CDCl₃) δ 165.8 (C=O), 150.7, 140.2, 136.8, 132.9, 132.0, 131.6, 131.5, 130.7, 129.6, 128.9, 128.2, 126.3, 122.1. Elemental Anal. Calcd. for C₃₂H₁₈Cl₄O₄ (608.29): C, 63.19; H, 2.98% Found: C, 63.14; H, 2.91%.

Bis(4'-(methylthio)-[1,1'-biphenyl]-4-yl) phthalate (**5c**)

Yield: 93%. Light yellow crystals. mp: 218-219°C. IR (KBr) cm⁻¹: 3012, 3008, 2921 (C-H stretching), 1731 (O-C=O-stretching), 1689 (C=O stretching), 1504 (C=C stretching). ¹H NMR (400 MHz, CDCl₃) δ 8.03 – 7.94 (m, 2H, Ar-H), 7.70 (d, *J* = 3.1 Hz, 2H, Ar-H), 7.57 (d, *J* = 2.1 Hz, 4H, Ar-H), 7.48 – 7.36 (m, 4H, Ar-H), 7.33 – 7.27 (m, 4H, Ar-

H), 7.12 (d, $J = 8.8$ Hz, 4H, Ar-H), 2.51 (s, 6H, 2CH₃). ¹³C NMR (101 MHz, CDCl₃) δ 165.8 (C=O), 155.3, 150.0, 138.7, 132.6, 131.9, 129.7, 128.0, 127.4, 127.1, 126.9, 123.4, 122.0, 15.8 (2CH₃). Elemental Anal. Calcd. for C₃₄H₂₆O₄S₂ (562.70): C, 72.57; H, 4.66% Found: C, 72.49; H, 4.65%.

Bis(4'-chloro-[1,1'-biphenyl]-4-yl) phthalate (5d)

Yield: 81%. White crystals. mp: 214-217 °C. IR (KBr) cm⁻¹: 3029, 2958, 2919, 2844 (C-H stretching), 1721 (O=C=O-stretching), 1689 (C=O stretching), 1483 (C=C stretching). ¹H NMR (400 MHz, CDCl₃) δ 8.03 – 7.95 (m, 2H, Ar-H), 7.70 (d, $J = 4.8$ Hz, 2H, Ar-H), 7.54 (d, $J = 8.3$ Hz, 4H, Ar-H), 7.47 – 7.41 (m, 4H, Ar-H), 7.40 – 7.36 (m, 4H, Ar-H), 7.29 (dd, $J = 11.6, 8.5$ Hz, 4H, Ar-H). ¹³C NMR (101 MHz, CDCl₃) δ 169.7 (C=O), 155.3, 139.2, 132.7, 129.0, 128.8, 128.3, 128.2, 128.1, 127.9, 122.0, 115.7. Elemental Anal. Calcd. for C₃₂H₂₀Cl₂O₄ (539.41): C, 71.25; H, 3.74% Found: C, 71.26; H, 3.76%.

Bis(4'-(methoxycarbonyl)-[1,1'-biphenyl]-4-yl) phthalate (5e)

Yield: 79%. Brown crystals. mp: 223-224 °C. IR (KBr) cm⁻¹: 3033, 3011, 2914, (C-H stretching), 1739 (O=C=O-stretching), 1687 (C=O stretching), 1593 (C=C stretching). ¹H NMR (400 MHz, CDCl₃) δ 8.01 (dd, $J = 6.1, 3.0$ Hz, 2H, Ar-H), 7.96 – 7.89 (m, 2H, Ar-H), 7.73 – 7.68 (m, 4H, Ar-H), 7.50 (d, $J = 8.8$ Hz, 4H, Ar-H), 7.31 (d, $J = 8.3$ Hz, 4H, Ar-H), 7.13 (d, $J = 8.7$ Hz, 4H, Ar-H), 3.93 (s, 6H, 2CH₃). ¹³C NMR (101 MHz, CDCl₃) δ 166.8 (C=O), 165.5 (C=O), 149.7, 144.3, 132.6, 132.0, 131.3, 130.2, 129.6, 127.2, 123.3, 119.4, 52.2 (2CH₃). Elemental Anal. Calcd. for C₃₆H₂₆O₈ (586.60): C, 73.71; H, 4.47% Found: C, 73.68; H, 4.45%.

Bis(3'-chloro-4'-fluoro-[1,1'-biphenyl]-4-yl) phthalate (5f)

Yield: 77%. Grey crystals. mp: 211-213 °C. IR (KBr) cm⁻¹: 3035, 2952, 2916, 2849 (C-H stretching), 1723, 1714 (O=C=O-stretching), 1684 (C=O stretching), 1481 (C=C stretching). ¹H NMR (400 MHz, CDCl₃) δ 8.13 – 8.10 (m, 2H, Ar-H), 7.96 (dd, $J = 5.7, 3.3$ Hz, 2H, Ar-H), 7.70 (d, $J = 3.2$ Hz, 2H, Ar-H), 7.69 (d, $J = 1.6$ Hz, 2H, Ar-H), 7.68 – 7.65 (m, 2H, Ar-H), 7.50 (d, $J = 8.8$ Hz, 4H, Ar-H), 7.09 (d, $J = 8.8$ Hz, 4H, Ar-H). ¹³C NMR (101 MHz, CDCl₃) δ 167.75 (C=O), 165.48, 149.65, 144.33, 132.62, 132.00, 131.31, 130.19, 129.56, 127.23, 123.30. Elemental Anal. Calcd. for C₃₂H₁₈Cl₂F₂O₄ (575.39): C, 66.80; H, 3.15% Found: C, 66.75; H, 3.17%.

Acknowledgements

The authors gratefully acknowledge the PCSIR (Ministry of Science and Technology), to access sophisticated equipment through the data repository of the scientific instrumentation development program initiated in 2021.

Supplementary Material

Supplementary data associated with this article are available in the Electronic Supplementary Material (ESI).

References

1. Kumar, R.; Verma, A.; Shome, A.; Sinha, R.; Sinha, S.; Jha, P. K.; Kumar, R.; Kumar, P.; Shubham; Das, S. *Sustainability* **2021**, *13*, 1-40.
<https://doi.org/10.3390/su13179963>

2. Huang, L.; Zhu, X.; Zhou, S.; Cheng, Z.; Shi, K.; Zhang, C.; Shao, H. *Toxins* **2021**, *13*, 495.
<https://doi.org/10.3390/toxins13070495>
3. Bang, S. Y.; Lee, K. J.; Koh, J. H.; Kang, M.-S.; Kang, Y. S.; Kim, J. H. *Ionics* **2008**, *14*, 143-148.
<https://doi.org/10.1007/s11581-007-0173-0>
4. Dong, X.; Long, M.; Liu, H.; Gao, L.; Xu, X.; Xia, X. *Appl. Polym. Sci.* **2023**, *140*, e53905.
<https://doi.org/10.1002/app.53905>
5. Chen, M.; Yang, B.; Zhang, J. *Appl. Polym. Sci.* **2024**, *141*, e56021.
<https://doi.org/10.1002/app.56021>
6. Arranz, F.; Chaves, M. S.; Gil, F. *Angew. Makromol. Chem.* **1980**, *92*, 121-132.
<https://doi.org/10.1002/apmc.1980.050920110>
7. Gümüş, M.; Babacan, Ş. N.; Demir, Y.; Sert, Y.; Koca, I.; Gülçin, İ. *Arch. Pharm.* **2022**, *355*, 2100242.
<https://doi.org/10.1002/ardp.202100242>
8. Miyaura, N.; Suzuki, A. *Chemical reviews* **1995**, *95* (7), 2457-2483.
<https://doi.org/10.1021/cr00039a007>
9. Güllüoğlu, M.; Erdogdu, Y.; Karpagam, J.; Sundaraganesan, N.; Yurdakul, Ş. *J. Mol. Struct.* **2011**, *990*, 14-20.
<https://doi.org/10.1016/j.molstruc.2011.01.001>
10. Mariappan, G.; Sundaraganesan, N. *J. Mol. Struct.* **2014**, *1063*, 192-202.
<https://doi.org/10.1016/j.molstruc.2014.01.064>
11. Elkaeed, E. B.; Mughal, E. U.; Kausar, S.; Al-ghulikah, H. A.; Naeem, N.; Altaf, A. A.; Sadiq, A. *J. Mol. Struct.* **2022**, *1270*, 1-14.
<https://doi.org/10.1016/j.molstruc.2022.133972>
12. Maqbool, T.; Younas, H.; Bilal, M.; Rasool, N.; Bajaber, M. A.; Mubarak, A.; Parveen, B.; Ahmad, G.; Ali Shah, S. A. *ACS Omega* **2023**, *8*, 30306-30314.
<https://doi.org/10.1021/acsomega.3c03183>
13. Balakit, A. A.; Makki, S. Q.; Sert, Y.; Uzun, F.; Alshammari, M. B.; Thordarson, P.; El-Hiti, G. A. *Supramol. Chem.* **2020**, *32*, 519-526.
<https://doi.org/10.1080/10610278.2020.1808217>
14. Shinde, R. A.; Adole, V. A.; More, R. A.; Jagdale, B. S.; Waghchaure, R. H.; Gurav, S. S.; Mali, S. N. *J. Mol. Struct.* **2025**, *1322*, 140313.
<https://doi.org/10.1016/j.molstruc.2024.140313>
15. Ojha, J. K.; Ramesh, G.; Reddy, B. V. *Chem. Phys. Impact.* **2023**, *7*, 1-8.
<https://doi.org/10.1016/j.chphi.2023.100280>
16. Basha, F.; Khan, F. L. A.; Muthu, S.; Raja, M. *Comput. Theor. Chem.* **2021**, *1198*, 113169.
<https://doi.org/10.1016/j.comptc.2021.113169>
17. Schrader, T.; Khanifaev, J.; Perlt, E. *Chem Commun.* **2023**, *59*, 13839-13842.
<https://doi.org/10.1039/D3CC04304E>
18. Suresh, C. H.; Remya, G. S.; Anjalikrishna, P. K. *Wiley Interdiscip. Rev. Comput. Mol. Sci.* **2022**, *12*, 1-31.
<https://doi.org/10.1002/wcms.1601>
19. Abdulridha, A. A.; Allah, M. A. A. H.; Makki, S. Q.; Sert, Y.; Salman, H. E.; Balakit, A. A. *J. Mol. Liq.* **2020**, *315*, 113690.
<https://doi.org/10.1016/j.molliq.2020.113690>
20. Fyfe, J. W.; Valverde, E.; Seath, C. P.; Kennedy, A. R.; Redmond, J. M.; Anderson, N. A.; Watson, A. J. *Chemistry—A European Journal* **2015**, *21* (24), 8951-8964.

- <https://doi.org/10.1002/chem.201500970>
21. Tùng, Đ. T.; Tuân, Đ. T.; Rasool, N.; Villinger, A.; Reinke, H.; Fischer, C.; Langer, P. *Adv. Synth. Catal.* **2009**, 351, 1595-1609.
<https://doi.org/10.1002/adsc.200900044>
22. Sieffert, N.; Wipff, G. *Dalton Trans.* **2015**, 44, 2623-2638.
<https://doi.org/10.1039/C4DT02443E>
23. Gökce, H.; Şen, F.; Sert, Y.; Abdel-Wahab, B. F.; Kariuki, B. M.; El-Hiti, G. A. *Molecules* **2022**, 27, 2193.
<https://doi.org/10.3390/molecules27072193>
24. Jamróz, M. H. *Spectrochim. Acta, Part A* **2013**, 114, 220-230.
<https://doi.org/10.1016/j.saa.2013.05.096>
25. Benbouguerra, K.; Chafai, N.; Chafaa, S.; Touahria, Y. I.; Tlidjane, H. *J. Mol. Struct.* **2021**, 1239, 1-11.
<https://doi.org/10.1016/j.molstruc.2021.130480>
26. Dege, N.; Gökce, H.; Doğan, O. E.; Alpaslan, G.; Ağar, T.; Muthu, S.; Sert, Y. *Colloids Surf., A* **2022**, 638, 128311.
<https://doi.org/10.1016/j.colsurfa.2022.128311>
27. Marcarino, M. O.; Zanardi, M. a. M.; Cicetti, S.; Sarotti, A. M. *Acc. Chem. Res.* **2020**, 53, 1922-1932.
<https://doi.org/10.1021/acs.accounts.0c00365>
28. Krivdin, L. B. *Molecules* **2021**, 26, 1-65.
<https://doi.org/10.3390/molecules26092450>
29. Sert, Y.; Çırak, Ç.; Uçun, F. *Spectrochim. Acta, Part A* **2013**, 107, 248-255.
<https://doi.org/10.1016/j.saa.2013.01.046>
30. Bozuyula, M.; Bayrakdar, A.; Sert, Y.; Kart, H. H.; Kart, S. O.; Manivannan, P.; Alma, M. H. *J. Comput. Chem.* **2025**, 46, e70098.
<https://doi.org/10.1002/jcc.70098>
31. Saidj, M.; Djafri, A.; Rahmani, R.; Belkafouf, N. E. H.; Boukabcha, N.; Djafri, A.; Chouaih, A. *Polycyclic Aromat. Compd.* **2023**, 43, 2152-2176.
<https://doi.org/10.1080/10406638.2022.2039238>
32. Kocakaya, Z.; Sert, Y.; Kocakaya, M.; Karatoprak, G. Ş.; İlgün, S.; Çadır, M. *J. Mol. Struct.* **2025**, 417, 126660.
<https://doi.org/10.1016/j.molliq.2024.126660>
33. Chermette, H. *J. Comput. Chem.* **1999**, 20, 129-154.
[https://doi.org/10.1002/\(SICI\)1096-987X\(19990115\)20:1%3C129::AID-JCC13%3E3.0.CO;2-A](https://doi.org/10.1002/(SICI)1096-987X(19990115)20:1%3C129::AID-JCC13%3E3.0.CO;2-A)
34. Sable, Y. R.; Adole, V. A.; Pithawala, E. A.; Amrutkar, R. D. *J. Sulphur Chem.* **2025**, 1-26.
<https://doi.org/10.1080/17415993.2025.2461582>

This paper is an open access article distributed under the terms of the Creative Commons Attribution (CC BY) license (<http://creativecommons.org/licenses/by/4.0/>)